The Journal of Experimental Biology 204, 1039–1052 (2001)
Printed in Great Britain © The Company of Biologists Limited 2001
JEB3140

A SHOT IN THE DARK: THE SILENT QUEST OF A FREE-FLYING PHONOTACTIC FLY

PIE MÜLLER* AND DANIEL ROBERT

Laboratory for Bioacoustics, Institute of Zoology, University of Zürich, Winterthurerstrasse 190, CH-8057 Zürich, Switzerland

*e-mail: piemue@zool.unizh.ch

Accepted 11 December 2000; published on WWW 26 February 2001

Summary

To reproduce, females of the parasitoid fly *Ormia ochracea* detect and localise a calling male cricket upon which they deposit their endoparasitic larvae. Calling male crickets are therefore subject to both sexual and natural selection by simultaneously attracting mates and phonotactic parasitoids. The possible strategy of song interruption employed by the cricket host to reduce his attractiveness to acoustic parasitoids was tested in the laboratory by examining the fly's phonotactic quest in response to synthetic cricket songs. Phonotactic flight trajectories were recorded in three dimensions with a stereo infrared video tracking system while the sound stimulus was controlled on-line as a function of the fly's position in space. Within a single flight, three distinct phases could be observed: a take-off phase, a cruising phase, during which course and altitude were rather constant, and a landing phase characterised by a spiralling descent towards the sound source. The flies showed remarkable phonotactic accuracy in darkness; they landed at a mean distance of 8.2 cm from the centre of the loudspeaker after a flight distance of approximately 4 m. The present data illustrate the fly's surprising ability to gauge the direction and distance of a sound source in three dimensions and, subsequently, to find it in darkness and silence.

Key words: acoustics, directional hearing, orientation, Diptera, parasite, *Ormia ochracea*, three-dimensional trajectory.

Introduction

The fly *Ormia ochracea* (Diptera, Tachinidae, Ormiini) is a larviparous parasitoid that relies on acoustic cues to detect and localise its host, singing male field crickets (Orthoptera, Gryllidae) (Cade, 1975; Walker, 1986). Since the presence of tympanal hearing was established in flies (Lakes-Harlan and Heller, 1992; Robert et al., 1992), the auditory capacity of *O. ochracea* has attracted some attention at the level of its anatomy (Robert et al., 1994; Edgecomb et al., 1995), neurophysiology (Robert et al., 1992), biomechanics (Miles et al., 1995; Robert et al., 1996; Robert et al., 1998) and behaviour (Walker, 1993; Wagner, 1995; Ramsauer and Robert, 2000). Constituting an evolutionary innovation within the order Diptera, these hearing organs are also endowed with an original method of sensing the direction of a sound source. Directional hearing is mediated by intertympanal mechanical coupling, a process that amplifies small acoustic cues into significant interaural time and amplitude differences (Miles et al., 1995; Robert et al., 1996; Robert and Hoy, 1998).

Previous research has shown that the gravid female fly – as a gregarious parasitoid – will deposit a clutch of larvae on a host, even when the host has already been parasitised. Larvae hatching from the first clutch develop into adults with a larger mass and body size (Adamo et al., 1995). Such adults also benefit from a higher survival rate (Adamo et al., 1995). Therefore, a female fly's reproductive success is expected to depend directly on her search efficiency which, in turn, is related to the fly's auditory capacity and to the cricket's acoustic conspicuousness. Several studies show that female flies prefer cricket calling songs with a longer chirp duration and a higher chirp amplitude (Wagner, 1995; Lehmann and Heller, 1998; Zuk et al., 1997). Hence, crickets would be expected to modify their song structure to reduce their conspicuousness, at least to parasitoid flies. Alternatively, crickets may also shift their diel activity pattern (Zuk et al., 1993) or interrupt their song completely in the presence of an acoustic parasitoid.

Little is known about the phonotactic behaviour of these gracile and elusive flies, mainly because they are crepuscular and nocturnal. Information about phonotactic flight paths may provide deeper insights into auditory perception in *O. ochracea* and may ultimately also help to explain the evolutionary constraints that resulted in the development of such small hearing organs. Flight trajectories were recorded to address questions about stimulus detectability and localisation and about the strategy of phonotactic orientation. The possible strategy of song interruption employed by the cricket host to reduce his attractiveness to acoustic parasitoids was also analysed.

In this study, the three-dimensional trajectories of free-flying phonotactic flies are described using finite helix fit analysis (Crenshaw et al., 2000) to investigate their approach strategy and search efficiency in the presence of synthetic cricket songs. The flight trajectories were recorded using a stereo video tracking system (Fry et al., 2000). The positional information was used to control, on-line, the sound stimulus as a function of the fly's actual position in space. Acoustic information alone is sufficient for the accurate localisation of the sound source. It is also demonstrated that, in the absence of previous experience, the fly *O. ochracea* is capable of locating a temporarily silent sound source in darkness.

Materials and methods

Animals

The flies, *Ormia ochracea* Bigot, used in the present study were reared in the Laboratory of Bioacoustics at the University in Zürich, Switzerland. The founder flies of our colony originated from Gainesville, Florida, USA, courtesy of Professor T. J. Walker. The flies were kept on a 16 h:8 h L:D photoperiod, at 26 °C, at a relative humidity of 60 % and provided with water and with Vita-Rich instant nectar for hummingbirds. If necessary, the concentration was 0.04 g ml^{-1} water. Experiments were performed only on gravid females because no positive phonotaxis occurs for other sex or age classes. Before the experimental procedure, the flies were cold-anaesthetised (4 °C) and individually colour-coded with water colour. This procedure does not influence the behaviour of the flies (Hischier, 1999).

Test arena

The behavioural experiments were conducted in an indoor room (length 6.8 m, width 4.9 m, height 4.0 m) with walls covered with high-frequency-absorbing foam (Maag Technic AG, type 1135). Inside this room, a flight cage (length 4.5 m, width 2.6 m, height 3.0 m) formed the actual test arena (Fig. 1A). To enhance the fly's contrast against the background for three-dimensional video tracking, the background was uniformly covered with black cotton sheets. To approach acoustic free-field conditions as closely as possible, the only objects placed in the test arena were a starting platform, two loudspeakers (each mounted in a cabinet covered with the same fabric as the background; length 30 cm, width 30 cm, height 8 cm) on the ground and two video cameras protruding through the roof (Fig. 1A).

General experimental procedure

A single fly was placed on the platform, and remained there motionless, until the test stimulus was presented. As soon as one of the two loudspeakers was turned on, the fly took off; it landed on the loudspeaker a few seconds later. The left and

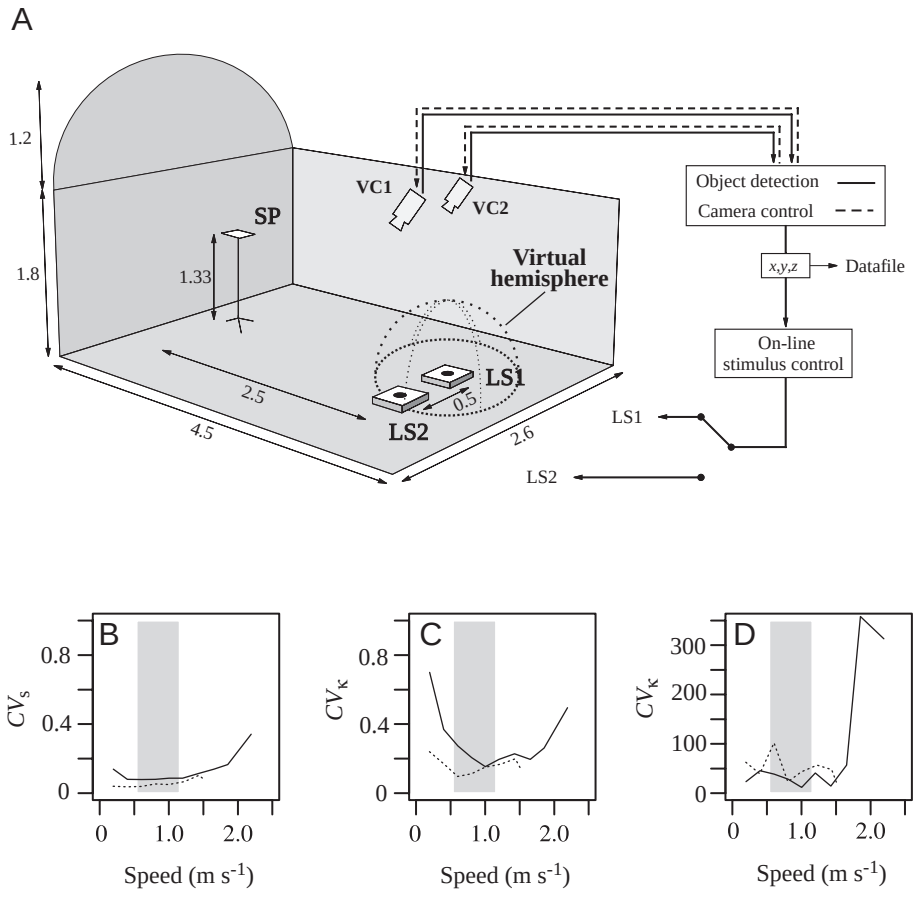

Fig. 1. Experimental arrangement for recording flight trajectories and on-line stimulus control, and estimates of data reliability. (A) Flight room with starting platform (SP) and two loudspeakers (LS1, LS2) each centred in a cabinet (length 30 cm, width 30 cm, height 8 cm). Flight trajectories were recorded with two pan-tilt infrared video cameras (VC1, VC2). Cartesian positional information (*x*, *y* and *z* coordinates; see Materials and methods) was saved on disk and streamed to a second computer to control the sound stimulus. Virtual surface areas and volumes, such as a loudspeaker-centred hemisphere, could be defined anywhere in the room. When the fly entered such a virtual space, predefined sound stimuli could be broadcast. Measurements are given in metres. (B-D) Calibration controls and data reliability, coefficients of variation (CV) for the finite helix fit (FHF) estimates (speed *s*, curvature κ and torsion τ; see Materials and methods) plotted as a function of the speed of the rotating light bulb used for calibrations. Measurements were taken above the loudspeaker cabinets (solid lines) or at the starting platform (dotted lines). Shaded areas show the range of the flies' flight speed observed for 100 different trajectories.

right loudspeakers were alternated for successive recordings to control for possible systematic errors in symmetrical experimental design. To investigate the reaction of the flies to stimulus interruption, the sound was switched off when the flying insect was located at six different radial distances (0.6–2.1 m) from the loudspeaker (see Table 2). Because flies would not fly for an unlimited number of replicates, samples were split into two cohorts each consisting of six individuals. Within a cohort, each experimental subject received three different treatments (see Table 2) and a control treatment in which sound was not interrupted during flight. To achieve the highest possible efficiency, the arrangement of treatments was balanced. Up to 10 trajectories were recorded for each possible combination of fly and treatment. Statistical analysis was performed on pooled data derived from flight trajectories to both loudspeakers.

Acoustic stimuli

To attract the flies to the loudspeaker, a model of the calling song of *Gryllus rubens* was generated using the program SoundEdit 16 (Macromedia) (16-bit resolution, 44.1 kHz sampling rate, WAVE file format). The trilling model song consisted of pulses of equal length with a pulse rate of 45 pulses s^{-1}. The duration of a single pulse was 13 ms, and pulses were separated by 9.2 ms gaps, with a 4.8 kHz carrier frequency. The sound pulse had a linear onset ramp of 2 ms and a linear offset ramp of 5 ms to mimic the cricket's natural song. Acoustic stimuli were broadcast from one of two loudspeakers (Radio Shack Super Tweeter, No. 40-1310B, 4 cm diameter; Fig. 1A). The sound files were played and their intensity controlled on-line by a custom-written program on a MacOS platform based on LabVIEW 5.0 (National Instruments). The intensities of the acoustic stimuli were measured with a TES 1352 sound level meter using its 'fast time' weighting function (calibrated with a Brüel & Kjær sound calibrator type 4231). Sound pressure levels (SPLs) in dB (re 20 μPa) were adjusted to 82 dB at 15 cm above the loudspeaker.

Data acquisition

Because *O. ochracea* is crepuscular and nocturnal (Walker, 1993) and, to exclude visual cues, all experiments were conducted under infrared illumination, providing illumination only to the camera tracking system. In total, an array of 17 lamps each comprising 100 infrared light-emitting diodes (LEDs; 875 nm peak wavelength) was mounted on the flight cage, generating light with an overall emission power of approximately 45 W.

Flight trajectories were recorded by two infrared-sensitive video cameras with pan-tilt optics (Sony LSX PT 1) (Fig. 1A). Camera tracking and trajectory data acquisition were achieved using the software Trackit Stereo (Fry et al., 2000) running on a Microsoft NT platform. In brief, this system permits the detection of a movable object by its contrast, in our case a light object on a dark background. The fly's actual flight path is reconstructed on the basis of snapshots from each camera that are sent to separate framegrabbers. A feedback algorithm predicts the fly's next position in space and steers the pan-tilt optics to keep the fly centred on the video frames. Using this system, the spatial position of a small object (millimetre range) can be accurately sampled at a frequency of 50 Hz. Because of the pan-tilt optics, tracking can be performed within a large volume (here approximately 20 m^3).

Sound stimulus control

The fly-tracking program allowed us not only to stream data to the hard disk but also to use this information to control the sound stimulus to be played as a function of the fly's position in space. Through a custom-built LabVIEW (National Instruments) user interface, the experimenter can link virtual surface areas, or volumes, of the experimental arena (such as a hemisphere, see Fig. 1A) with specific sound stimuli (WAVE sound files). Multiple areas of different shapes and dimensions linked to different sound stimuli can be freely arranged in space and combined, using Boolean logic, on the computer screen. Thus, when the fly intersects such a virtual area, or enters a volume, a corresponding and predetermined sound stimulus is presented. This application allowed us to study the sensory perception and spatial orientation of a freely moving animal without sacrificing the experimental manipulation of the stimulus.

Estimation of tracking errors

The spatial accuracy of the tracking method depends on the speed of the moving object and its position relative to the cameras (also resulting in different object resolutions and angular velocities of the movable optics). Tracking errors were estimated by tracking a control signal consisting of a light bulb mounted on a carousel (0.3 m radius) that rotated at different angular speeds in the horizontal plane. The carousel was mounted at 1.33 m above the ground either at the starting platform or above the loudspeakers. The coherence of the tracking system was assessed using the finite helix fit (FHF) technique (after Crenshaw et al., 2000). This technique is based on the geometry of three-dimensional curves, whereby a three-dimensional trajectory is completely described by its translational velocity $\mathbf{V}$ (with a speed s), curvature κ and torsion τ (see below and Fig. 2A). The coefficient of variation (standard deviation/mean) was calculated for all three estimates and plotted as a function of the light bulb's speed to illustrate that, within the range of the fly's velocity (shaded areas in Fig. 1B–D), the errors of measurement are acceptable. In contrast to speed and curvature, the estimates for torsion revealed rather high coefficients. Theoretically, the carousel's circular motion is two-dimensional, encompassing constant, non-zero speed and curvature, but no torsion (i.e. mean τ=0; no helical motion). The measured positional data points, however, may differ slightly from the theoretical circular trajectory. As a consequence, even the smallest jitters will give rise to a large coefficient of variation (Fig. 1D).

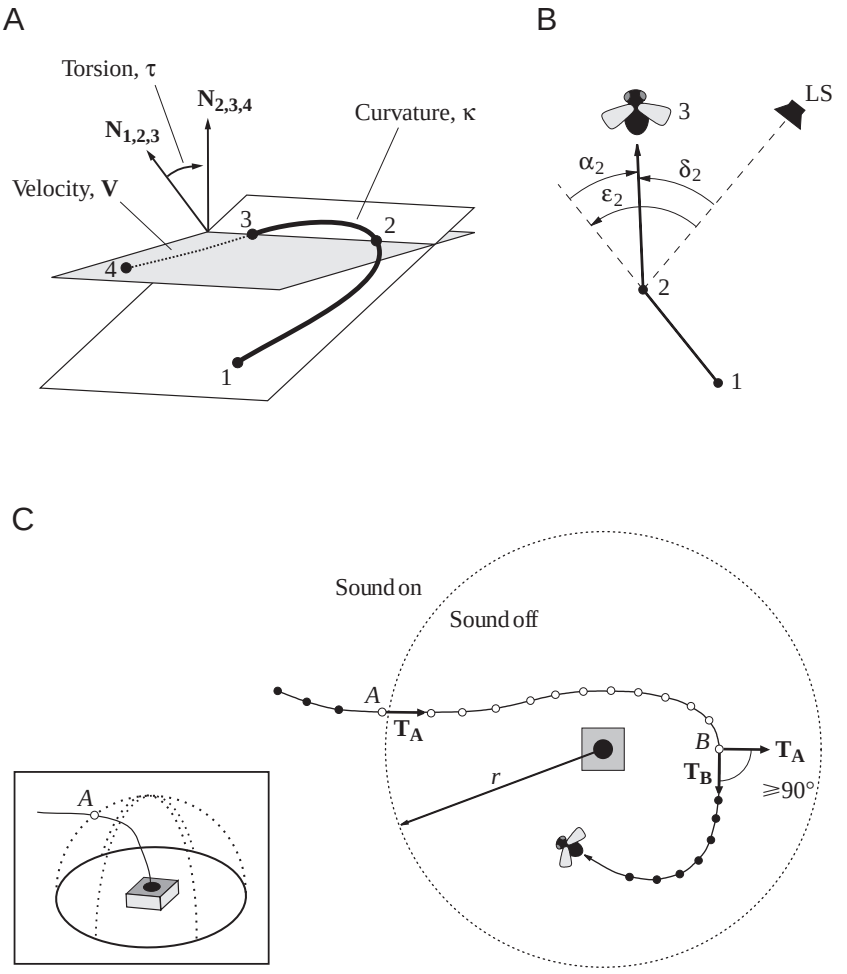

Fig. 2. Definitions of the variables describing the flight trajectories. (A) Estimation of velocity (**V**), curvature κ and torsion τ by the finite helix fit (FHF) technique. τ is defined as the angular change between the subsequent normal vectors $\mathbf{N_{1,2,3}}$ and $\mathbf{N_{2,3,4}}$ of the planes defined by the points 1–3 and 2–4, respectively. (B) Actual angle α_i, error angle ε_i and residual angle δ_i at time t_i. In this case, angles are estimated at t_2 using the positional information over time t_1–t_3 (at positions marked 1, 2 and 3). LS, loudspeaker. (C) Flight trajectory penetrating the surface of a virtual hemisphere of radius r (dotted circle) centred on the loudspeaker (grey box). Intersection of the flight path with this hemisphere triggered stimulus interruption. Inset: three-dimensional view of the fly's trajectory intersecting the surface of the virtual hemisphere at position *A*. The vector tangential to the flight path at position *A* ($\mathbf{T_A}$) constitutes the orientation reference at the time of stimulus interruption. Vector $\mathbf{T_B}$ defines the position at which $\mathbf{T_A}$ has turned by 90° or more. Position *B* is defined as the position of reversal, at which the fly initiates its spiralling descent towards the loudspeaker. Time delay and distance to reversal ($\mathbf{T_A}$–$\mathbf{T_B}$) were calculated along the three-dimensional data points between *A* and *B* (open circles).

Analysis of the flight trajectory

Data processing was performed using the statistical software package R 1.0 (General Public Licence) running on a LINUX platform. Analyses of variance (ANOVAs) for repeated measures were computed in S-Plus 4.3 (MathSoft, Inc.) using the rm.tools package (Azzalani and Chiogna, 1995) running on a UNIX platform.

The three-dimensional trajectories were analysed using the FHF technique (Crenshaw et al., 2000), whereby a three-dimensional trajectory is completely described by its translational velocity **V**, curvature κ and torsion τ. **V** can be decomposed into speed magnitude *s* and direction **T**. **T** is the unit tangent vector that points in the direction of motion and has a magnitude of 1. All these variables were estimated directly from the discretely sampled (50 Hz) positional data (Fig. 2A). All estimates were computed by choosing an optimal 12-point window (see Crenshaw et al., 2000). Here, vectors are presented in bold upper case font (e.g. **V**) and scalars in lower case font (e.g. *s*). In addition, as a description of course direction with respect to the broadcasting sound source, angles and path lengths were computed on the basis of Cartesian positional information (*x*, *y*, *z* coordinates).

The following angles describing the flight behaviour at a given time t_i (Fig. 2B) were calculated. α_i, the actual angle expressing the change in flight direction, is measured between two successive time intervals t_i and t_{i+1}. From the fly's point of view, positive values indicate a turn to the right and negative values a turn to the left. ε_i, the error angle, is the angular deviation of the fly's instantaneous direction from that to the active loudspeaker. The sign rule is the same as above. δ_i, the residual angle or 'true' error angle, is the difference between the error angle ε_i and the actual angle α_i. δ_i is the amount of angular distance that the fly has not corrected at time t_i.

To quantify the flight behaviour in summary, we evaluated the angular density function of ε_i by means of a non-parametric estimate using a Gaussian kernel over all positions of each single flight trajectory. From each distribution, the half-width (i.e. width at half-height of the peak) was estimated. The mean values from 10 successive trials per animal were then compared among individuals.

To obtain a more detailed description of the fly's approach as a function of its distance from the active loudspeaker, distances from the loudspeaker were divided into 12 intervals (interval length 0.25 m). Half-widths for ε for each corresponding interval were calculated. To express how tortuous the flight path is as a function of distance from the sound source, the mean vector length for α (Batschelet, 1981)

was computed over all intervals of individual flights. This variable ranges between 0 and 1. A value of 0 means that all directions are equally represented, a value of 1 indicates that the fly always flew in the same direction.

Orientation after stimulus interruption

The loudspeaker was switched off when the fly entered a virtual hemisphere centred on the loudspeaker (Fig. 2C inset). Persistence in orientation was quantified as the time (and distance) between the tangent $\mathbf{T_A}$ aligned with the flight direction at stimulus interruption and the tangent $\mathbf{T_B}$ at which the flight trajectory had turned by 90° (Fig. 2C). Estimates of time and distance took into account the system's reaction time, a computational delay measured to be 38.1±6.5 ms (mean ± S.D., N=9). Differences in landing accuracy and persistence of orientation between treatments were analysed using ANOVA for nested models (Venables and Ripley, 1997). To test for dependence of the flight path geometry (speed s, curvature κ and torsion τ) and other flight variables (absolute error angle $|\varepsilon|$ and flight altitude z) on landing accuracy and persistence of orientation upon stimulus interruption, multiple linear regression analyses were performed. Unless stated otherwise, the level of significance was set at 0.05.

Results

General description of the phonotactic flight path

Gravid female flies placed on the starting platform did not initiate flight before a sound stimulus was broadcast from one of the two loudspeakers. Upon onset of the simulated cricket song, the fly took off within a few seconds and approached the active loudspeaker. An example of a typical phonotactic flight trajectory is documented in Fig. 3A. Within a single flight,

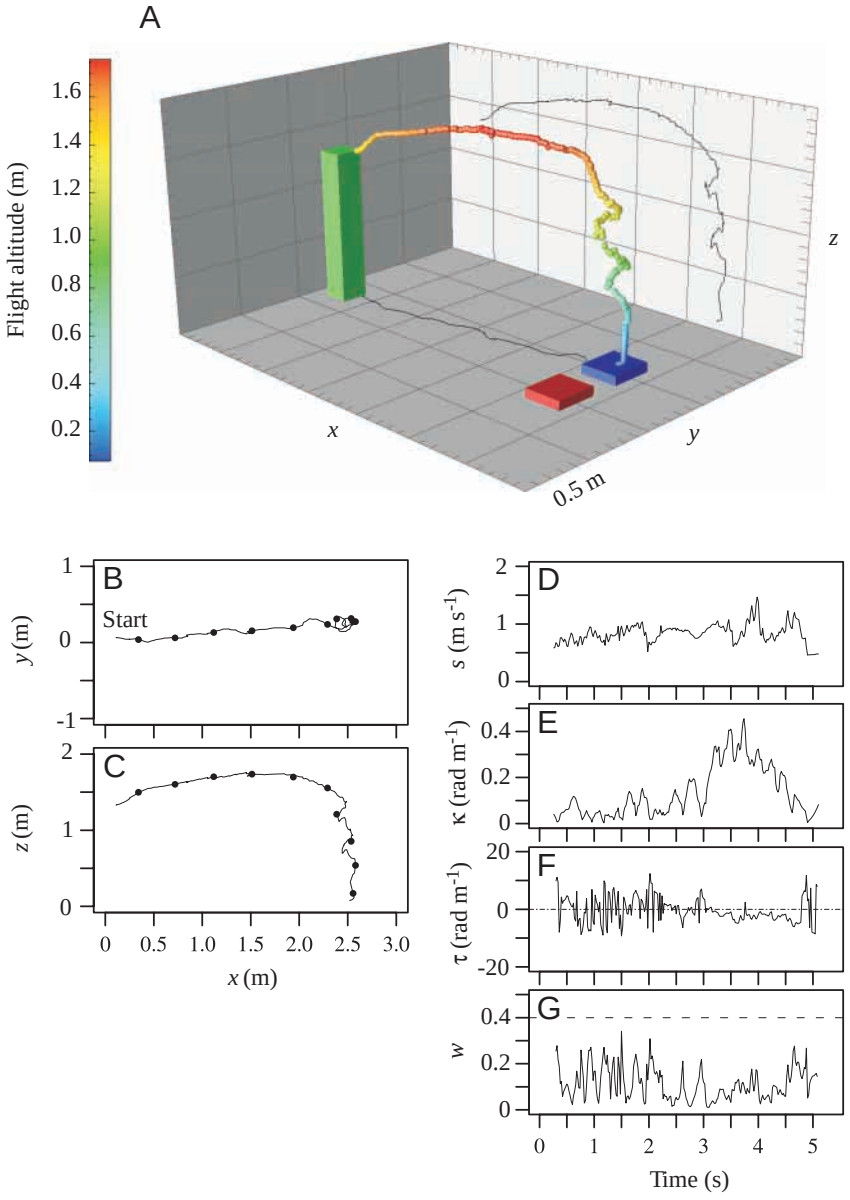

Fig. 3. Three-dimensional flight trajectory and finite helix fit (FHF) analysis of a single phonotactic flight during continuous stimulus presentation (carrier frequency 4.8 kHz, pulse rate 45 pulses s^{-1}, 82 dB SPL at 15 cm above the loudspeaker). (A) Taking off from the starting platform (green column), the fly landed on the broadcasting loudspeaker (blue box). Colour-coded symbols (x,y,z data points) represent the fly's position at 20 ms intervals as a function of flight altitude (z axis). Black lines show two-dimensional projections onto the xy and xz planes (i.e. top and side views, respectively). (B,C) Two-dimensional projections, as in A, with 0.5 s time markers (black circles). 'Start' marks the beginning of the trajectory. (D–G) Estimated speed s, curvature κ, torsion τ and dimensionless window size w as a function of time.

three distinct phases can be distinguished: a take-off phase, a cruising phase and a landing phase. Inspection of the flight trajectory in a three-dimensional representation reveals that the fly first gains altitude (take-off phase) and then approaches the sound source along a slightly meandering path (cruising phase). Closing in on the sound source, the fly initiates a spiral descent to the loudspeaker (landing phase) (Fig. 3A). These three distinct flight phases are clearly visible from the side and top views (ground and back wall projections in Fig. 3A and Fig. 3B,C). To read the trajectory as a function of time, 0.5 s interval time markers (filled circles) are drawn along the trajectory (Fig. 3B,C).

The FHF estimates of speed s (Fig. 3D), curvature κ (Fig. 3E) and torsion τ (Fig. 3F) completely describe the trajectory of Fig. 3A. During the first 0.5 s, the fly increases s from 0 m s^{-1} to approximately 0.75 m s^{-1}, reflecting the high acceleration of the take-off phase. From then on, speed varies between 0.5 and 1 m s^{-1} during the cruising phase (time 0.5–3 s). This is in accordance with the mean velocity of 0.92±0.06 m s^{-1} (mean ± S.E.M.) measured over a sample of 100 trajectories (N=26 727 positional data points) from 10 different individuals. Two velocity peaks occur during the landing phase at approximately 4 and 4.5 s (Fig. 3D). These peaks coincide with trajectory positions at which the fly passes over the loudspeaker and swiftly turns back to enter the diving spiral (see Fig. 3C). The take-off and cruising phases are accompanied by small variations in κ. As the fly switches from the cruising to the landing phase after approximately 3 s of flight, κ increases substantially (Fig. 3E). τ shows rather noisy variation except during the helical trajectory of the landing phase (Fig. 3F), where it consistently takes negative values, corroborating the distinct left-handed helical turn of the flight path (Fig. 3A). Note that κ and τ are given in rad m^{-1}, and not in units of time. In agreement with Crenshaw et al. (Crenshaw et al., 2000), reliable estimates for s, κ and τ are obtained when the 'dimensionless window size' w remains well below 0.4 (Fig. 3G). w expresses the fraction of one rotation of the flight trajectory spanned by two consecutive points at which the variables are estimated. Like the Nyquist critical sampling frequency, aliasing occurs when w is equal to or exceeds 0.5 (see Crenshaw et al., 2000).

Even though w remained below 0.4, several points of caution need to be taken into account. First, w is computed on the basis of estimated s, κ and τ and is therefore subject to systematic errors. Second, the use of 12-point spacing makes the estimates, in effect, an average over a large portion of the flight trajectory. Therefore, sharp transients tend to disappear. Third, in the absence of helical motion, τ tends to become noisy. In this situation, the coefficient of variation for τ becomes very high, i.e. the standard deviation (S.D.) becomes much larger than the mean. This effect can also be seen in control measurements (Fig. 1D) with the circling carousel, for which the theoretical mean value of τ is 0 rad m^{-1}.

Variation in the phonotactic trajectories

Inter-individual variability in the phonotactic trajectories is

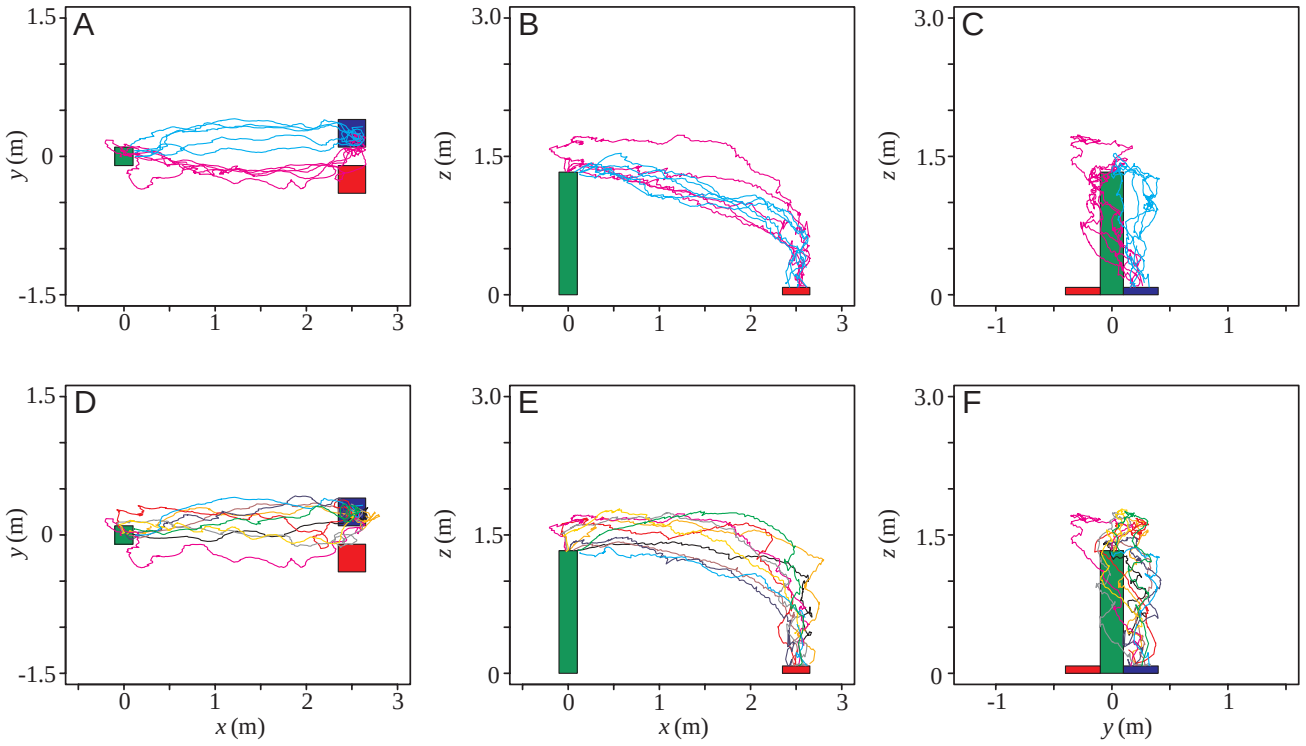

Fig. 4. Inter- and intra-individual variability of flight trajectories. Projections onto the *xy*, *xz* and *yz* planes (top, side and frontal views, respectively). Green rectangle: starting platform. Blue box: active loudspeaker. Red box: silent loudspeaker. (A–C) Phonotactic behaviour of two flies, five flight trajectories for each (pink and blue). (D–F) Flight trajectories from 10 different flies (one colour each).

greater than that of single individuals (Fig. 4). A comparison of flight trajectories from a single individual reveals highly stereotypical flight paths (Fig. 4A–C). Flight trajectories are self-similar in that, for example, one fly (pink lines) showed a consistent left-handed bias when approaching the sound source. Another fly (blue lines), however, repeatedly flew more directly towards the loudspeaker. The variability in flight pattern among individuals is even more conspicuous when single trajectories from different individuals recorded under identical experimental conditions are compared (N=10 animals, Fig. 4D–F). The fact that intra-individual variability is low also permits the pooling of data from the same individual for further data processing.

The computed half-widths from the angular distributions (Fig. 5A–C) yield significantly smaller actual angles than error angles (one-sample Wilcoxon test, one-sided, P<0.001, N=10 animals, n=100 trajectories). This difference is very pronounced in the *xy* projection (top view; Fig. 5B). This indicates that, for the entire flight bout, the flies correct their flight trajectory towards the loudspeaker by an angle α consistently smaller than the angle required for perfect alignment (ε). In addition, the angular distribution of the residual angles δ is almost equal to that of ε (Fig. 5A). Mean values for the half-widths of α are 51.0±2.6° (mean ± S.E.M., for the three dimensions), 16.0±1.0° (mean ± S.E.M., *xy* projection) and 30.3±1.2° (mean ± S.E.M., *xz* projection). The corresponding values for the distributions of ε are 56.5±1.1°, 53.3±1.4° and 70.0±4.3° (means ± S.E.M.). The half-widths of δ (not shown) are almost identical to those of ε.

Further analysis revealed that α and ε also vary as a function of the three flight phases (take-off, cruising and landing; Fig. 5D–F). Between 3 and 2.5 m from the loudspeaker (take-off phase), the half-width for ε decreases dramatically from initial high values (up to 225° in the three-dimensional computation). As the flies approach the sound source (approximately 2.5–1.25 m; the cruising phase), the half-widths increase steadily for successive intervals. From 1.25 to 0 m, the half-widths increase almost exponentially (landing phase), an indication of the flies' spiralling descent towards the loudspeaker.

Instantaneous flight direction, expressed as the mean vector length of α, behaves as a mirror image of the half-width for ε. In brief, higher values of α are reached whilst half-widths for ε are narrow, and *vice versa*. A rapid increase in α occurs at a distance of 3–2.5 m from the sound source (take-off phase). Flight direction increases steadily during the cruising phase, to become less stable as the flies close in on the loudspeaker (1.25–0 m intervals).

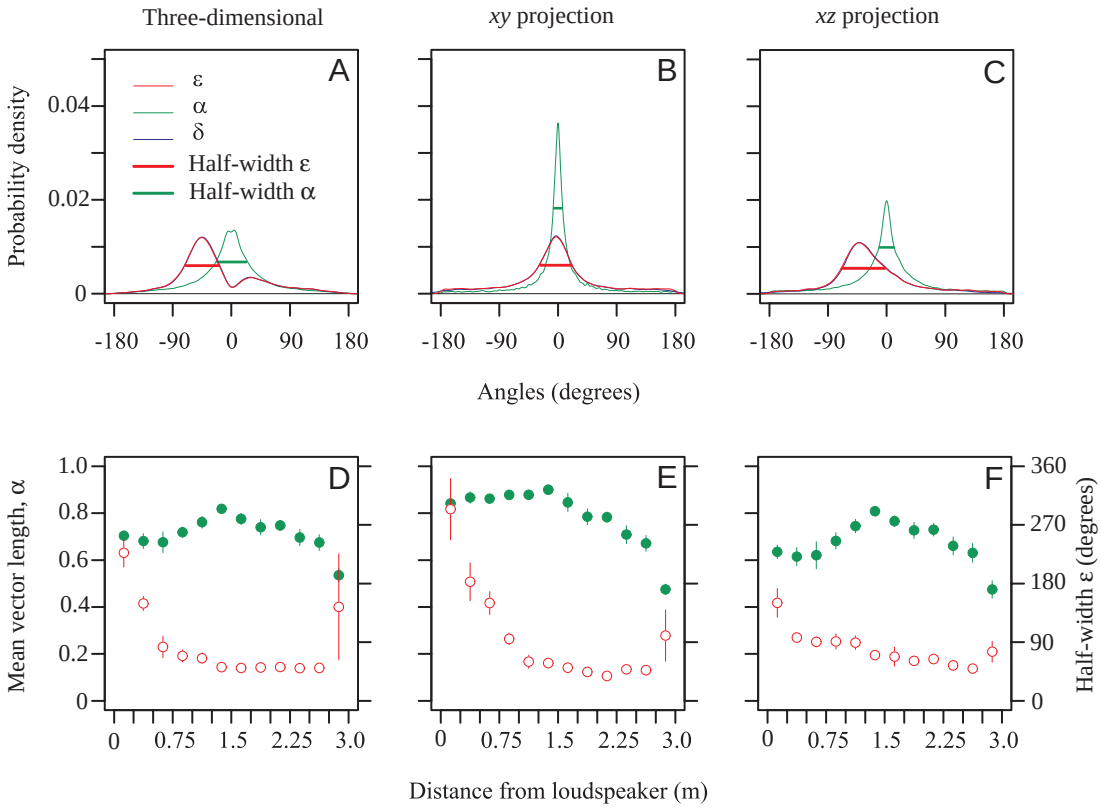

Fig. 5. Angular distributions and derived variables (N=10 individuals, n=100 trajectories). (A) Angular distribution of actual angles α, error angles ε and residual angles δ (see Fig. 2B for definitions) in all three dimensions. Half-widths of angular distributions are indicated by thick horizontal bars. (B,C) Angular distributions (as in A) computed for *xy* projections (B; top view) and *xz* projections (C; side view). (D–F) Length of the mean vector for α (brown open circles) and half-width for ε (green filled circles) plotted as a function of the fly's distance from the loudspeaker, shown for all three dimensions (D), for *xy* projections (E) and for *xz* projections (F). Values are means ± S.E.M.

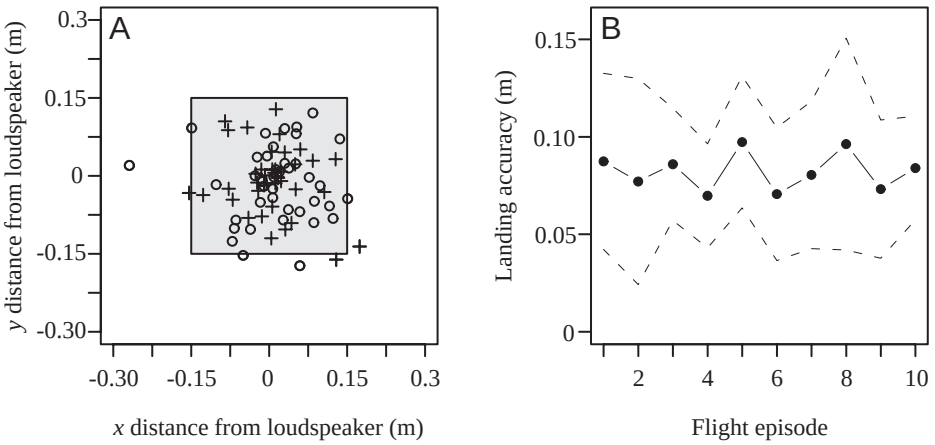

Fig. 6. Landing accuracy of phonotaxis in response to a continuous sound stimulus. (A) Landing positions (N=10 animals, n=80 landings). Shaded area: loudspeaker cabinet. Open circles: landings on the left-hand loudspeaker. Crosses: landings on the right-hand loudspeaker. (B) Landing accuracy (measured as the landing distance from the centre of the loudspeaker) as a function of 10 consecutive phonotactic flights (same data as plotted in A). The broken lines are the 95 % confidence limits.

Landing accuracy

The success of the fly's search can be assessed by the accuracy of the landing position (measured as the landing distance from the centre of the loudspeaker). In total, 80 flight trajectories were examined for landing accuracy (Fig. 6A). The flies land surprisingly close to the centre of the loudspeaker (radius 4 cm), at a mean distance of 8.2±0.6 cm (mean ± S.D.). When landings are investigated sequentially (Fig. 6B), landing accuracy shows no improvement over time. ANOVA for repeated measures yields no statistically significant differences (P=0.296): previous experience does not improve landing accuracy. In agreement with landing accuracy, the distribution of ε does not change over time (ANOVA for repeated measures, P=0.728).

Stimulus interruption

These experiments entail the interruption of the sound stimulus as the fly's phonotactic trajectory enters the virtual hemisphere centred on the loudspeaker (Fig. 2C; for example at 1.8 m from the sound source). Remarkably, upon stimulus interruption, the fly continued her flight course to land near the initially active loudspeaker (Fig. 7A). In this situation, the transition between the cruising and landing phases is less distinct. Compared with the standard situation (as seen in Fig. 3), the landing phase is characterised by broader helical loops (Fig. 7B,C). In this example, s initially and transiently increases and then decreases approximately 1 s after stimulus interruption (Fig. 7D). Flight speed remains low until landing, contributing to the overall longer flight duration observed in stimulus interruption experiments (two-sample Wilcoxon test, one-sided, P<0.001, n=395 trajectories). Throughout the flight, κ remains rather low (Fig. 7E, compare Fig. 3E), with regular variations reflecting the smooth and ample turns (after 3 s of flight onwards). This stands in contrast to the distinct increase in κ observed after 3 s of flight in the standard phonotactic flight (Fig. 3E). The absence of coherent helical motion, during the landing phase in particular, also results in a very noisy variation of τ (Fig. 7F). w consistently remains below the critical value of 0.4 for the entire flight duration (Fig. 7G), indicating the reliability of the FHF estimates and the absence of aliasing.

Landing accuracy after stimulus interruption

On the basis of 74 recorded landings, landing accuracy decreased for increasing distances of stimulus interruption (ANOVA, P<0.0001) (Fig. 8A,B). Notably, landings occurring after long interruption distances tended to undershoot the position of the sound source (Fig. 8A). For stimulus interruption distances greater than 1.5 m, the phonotactic response degraded (Fig. 8B), so that some flies were no longer able to find the inactivated sound source, instead flying to the walls of the flight cage or cruising past the silent loudspeaker in a straight line. When stimulus interruption took place during the take-off phase, the flight trajectories became randomly distributed in the arena (data not shown).

As shown above, the geometry of the flight trajectory changes as the fly approaches the sound source (Figs 3–5). Therefore, the dependence of landing accuracy on several flight variables (speed s, curvature κ, torsion τ, flight altitude z and absolute error angle |ε|) was tested. Multiple linear

Table 1. *Coefficients of multiple linear regression analysis for landing accuracy and persistence of orientation*

	Landing accuracy		Persistence of orientation	
	Estimate	P	Estimate	P
Intercept	0.625	<0.01	–2.494	<0.0001
s	–0.010	NS	2.354	<0.0001
κ	–0.730	NS	–5.936	<0.0001
τ	–0.005	NS	0.014	NS
z	–0.475	NS	–0.047	NS
|ε|	0.000	NS	–0.007	NS
r^2	0.065	NS	0.162	<0.0001

For landing accuracy, n=74 flight trajectories were sampled from N=12 flies.

For persistence of orientation, n=254 trajectories were recorded from N=12 flies.

Persistence of orientation is defined here as the distance to reversal (see Fig. 2C).

s, speed; κ, curvature; τ, torsion; z, flight altitude; |ε|, absolute error angle; NS, not significant.

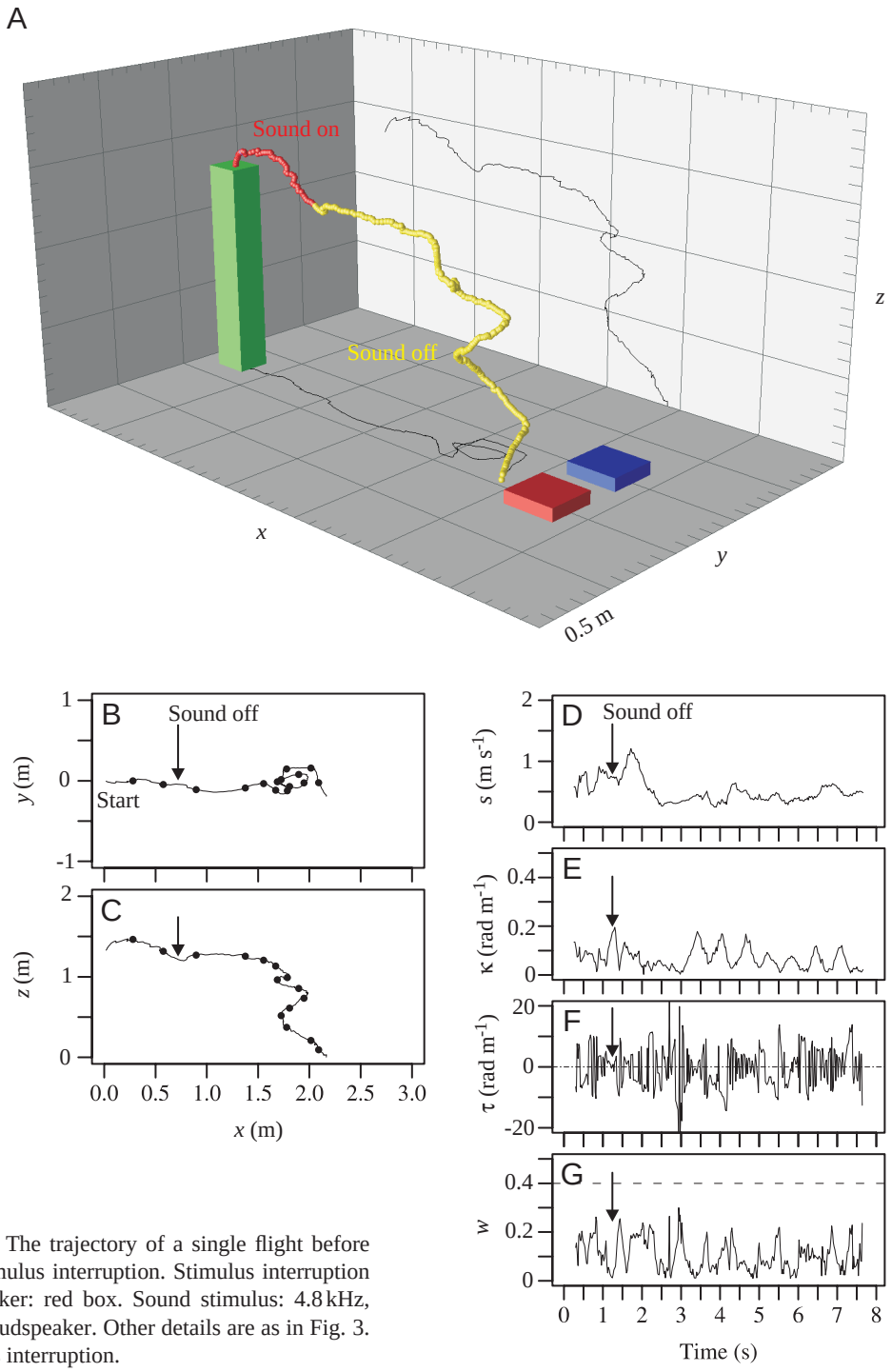

Fig. 7. Stimulus interruption experiment. (A) The trajectory of a single flight before (red symbols) and after (yellow symbols) stimulus interruption. Stimulus interruption distance, 1.8 m. Temporarily active loudspeaker: red box. Sound stimulus: 4.8 kHz, 45 pulses s^{-1}, 82 dB SPL at 15 cm above the loudspeaker. Other details are as in Fig. 3. Arrows in B–G indicate the instant of stimulus interruption.

regression analysis of all interrupted flight trajectories established that landing accuracy is not predicted by these variables (Table 1). In other words, landing accuracy is independent of the geometry of the trajectory.

Persistence of orientation after stimulus interruption

Flies respond differently depending on their position in space at the time of stimulus interruption (Figs 8, 9). Upon interruption far away from the sound source, the fly's orientation persists for longer. Stimulus interruption far (up to 1.8 m) from the loudspeaker does not prevent the fly from landing remarkably close to it (Figs 8A, 9A). To achieve this, the fly continues the same flight course and initiates the spiralling descent at the appropriate time and place, landing relatively close to the loudspeaker. In contrast, a fly already close to the loudspeaker at the time of stimulus interruption starts her spiralling descent earlier. Remarkably, these landing manoeuvres are initiated at a time when sound cues are absent.

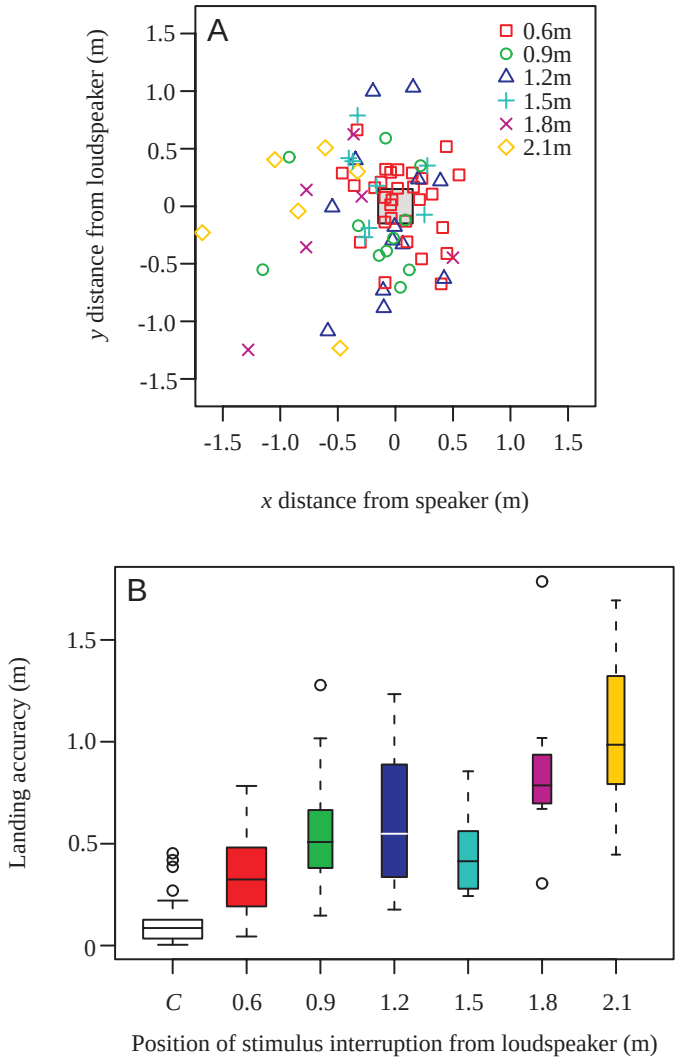

Fig. 8. Landing accuracy as a function of the distance of stimulus interruption. (A) Top view of the landing positions for different distances of stimulus interruption; 74 landing positions were recorded from six flies per treatment. The grey box indicates the loudspeaker position to scale. (B) Summary statistics of the landing accuracy measured by the landing distance from the loudspeaker (n=154 landings). The widths of the box plots vary according to the sample size within each category (N=6–80), and colours correspond to treatments in A. The centre line through each box represents the median. Boxes represent the interquartile distance (IQD). The whiskers extend to the extreme values of the data (i.e. ±1.5×IQD from the median). Open circles indicate possible outliers. *C*, control.

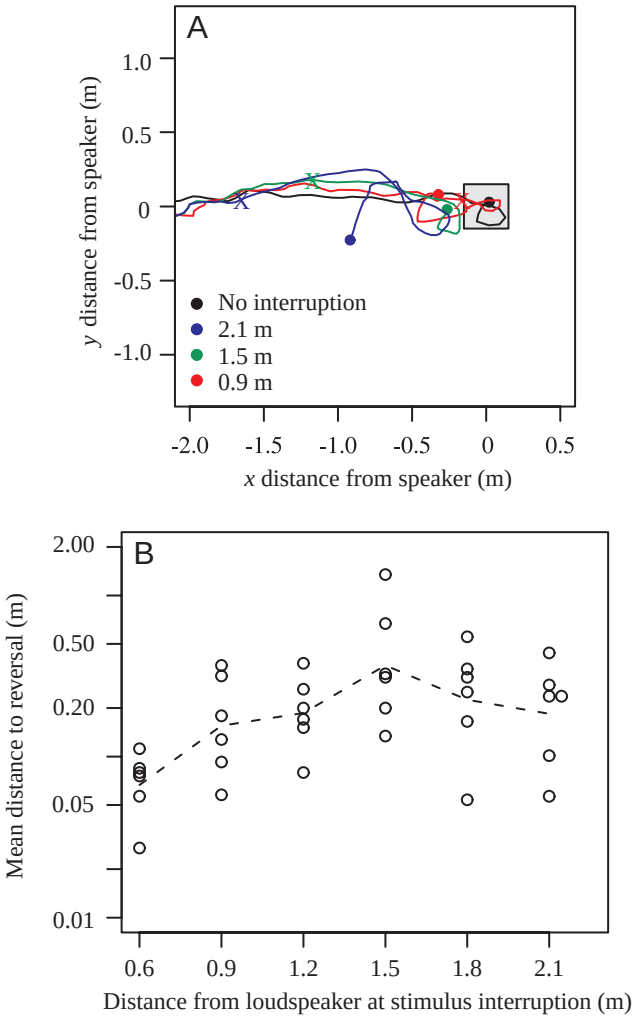

Fig. 9. Behavioural response to stimulus interruption at different distances from the loudspeaker. (A) Phonotactic and landing trajectories of a single fly for three different distances of stimulus interruption. Landing positions are shown by filled circles. Crosses indicate the fly's position at the time of stimulus interruption. The grey box shows the loudspeaker platform to scale. (B) Distance to reversal (see Fig. 2 and Materials and methods) for different distances of stimulus interruption (mean values for individual flies; n=254 trajectories in total). The broken line connects the means of each category (see Table 2). Note that the statistical analysis required a logarithmic transformation of the dependent variable.

In effect, the earlier the stimulus is interrupted, the less accurate the landing becomes (Fig. 8A,B).

In total, 254 trajectories, 3–10 in each treatment from 12 flies, were recorded and evaluated with respect to persistence of orientation after stimulus interruption (Tables 1, 2; Fig. 9B). The persistence of orientation can be measured either as the time elapsed between stimulus interruption and trajectory reversal or as the distance flown to reversal. Values for time and distance (Table 2) are highly correlated (r=0.972, P=0.001). Therefore, only values for distance to reversal are considered in the following. Fig. 9A,B illustrates the change in the fly's phonotactic behaviour as a function of stimulus interruption. In most cases, flies landed relatively close to the loudspeaker despite stimulus interruption. The distance to reversal in the trajectory (as defined in Fig. 2C) was significantly (ANOVA, P=0.003) shorter when stimulus interruption occurred close to the loudspeaker (e.g. 0.6 m) (Fig. 9B). In contrast, flies tended to maintain their flight course when stimulus interruption occurred further from the loudspeaker. In other words, stimulus interruption does not elicit the spiralling trajectory indicative of landing. For stimulus interruptions at 1.8–2.1 m, the flies maintain their

Table 2. *Mean distance to stimulus at interruption, time delay and distance to reversal under different stimulus conditions*

Distance of stimulus interruption (m)	Distance to reversal (m)	Time delay (s)	Fly cohort	*N* (individuals)	*n* (trajectories)	*n* (left arena)
0.6	0.07	0.07	A	6	41	6
0.9	0.16	0.15	B	6	43	9
1.2	0.18	0.19	A	6	42	11
1.5	0.37	0.41	B	6	47	9
1.8	0.23	0.28	A	6	34	7
2.1	0.18	0.25	B	6	47	5

In total, n=254 trajectories from N=12 flies were recorded.

Within a cohort (A or B), each animal received three different treatments and a control treatment in which sound was not interrupted during flight. Such a cohort forms an experimental block.

Reversal is where the fly initiates the spiralling descent towards the loudspeaker (see Fig. 2C).

course and delay their descent until relatively close to the loudspeaker. Hence, the spiralling descent does not occur until a certain distance has been flown (or after a certain time delay) after stimulus interruption. Stimulus interruption between 0.6 and 1.5 m from the loudspeaker leads to spiralling when the flies have flown an appropriate time or distance to initiate their oriented descent towards the silent loudspeaker. At interruption distances greater than 1.5 m, landing accuracy decreases but an oriented flight trajectory persists, eventually leading towards the sound source.

The influence of five flight trajectory variables (s, κ, τ, z and $|\varepsilon|$) on the persistence of orientation was also assessed by multiple linear regression analysis. This analysis established complete independence between all variables except for s and κ (Table 1), which exert an influence, although weak, on the persistence of orientation ($\log y = -2.913 + 2.515s - 6.393\kappa$; r^2=0.14, P<0.0001). The reduced model indicates that orientation persistence is more robust for flies moving at high speed and following a straighter trajectory (low κ).

Discussion

The present analysis documents how free-flying acoustic parasitoid flies (*Ormia ochracea*) approach a sound source. In the absence of visual or olfactory cues, the flies show remarkable landing accuracy, often landing within a few centimetres of the sound source. The behavioural evidence demonstrates that sound alone is sufficient for successful phonotaxis, but also that these cues are not necessary at all times. Most surprisingly, orientation towards the sound source persists after stimulus interruption, illustrating the fly's ability to pursue her goal even in the prolonged absence of acoustic cues. This finding raises interesting questions about the navigational mechanisms used by the fly in her silent quest.

The path to the goal

The phonotactic trajectories of *Ormia ochracea* do not follow the shortest distance between the release point and the loudspeaker. In fact, the trajectories are always curvilinear, vary little in altitude during the cruising phase and undergo a steep descent close to the sound source. This finding corroborates observations from acoustic trapping in the field (T. J. Walker and D. Robert, personal observations). Arguably, cruising at a particular altitude (1.5–2 m above ground) may improve the fly's ability to detect and locate her host because both amplitude and directional sound cues suffer close to the ground (Michelsen and Rohrseitz, 1997; Römer, 1998).

No improvement with experience

The accuracy of phonotaxis, measured as the distance between the landing position and the centre of the loudspeaker, did not improve for successive flight sequences. Naive females were able to detect and locate the sound source equally as well as experienced females, suggesting that phonotaxis is independent of previous experience (or operant learning of spatial features). In principle, learning about the position of a cricket could greatly improve the efficiency of the phonotactic search. In the present situation, however, such a strategy would be of little benefit for several reasons. First, the cricket hosts of *O. ochracea* are highly mobile during their calling period. Second, to learn about the cricket's position, the fly would presumably require the experience of flying to it at least once. Such experience is shown here not to be necessary. Third, visiting the same host twice would imply self-superparasitism, a strategy that makes little sense since secondary, or multiple, infestations result in an overall lower reproductive success (Adamo et al., 1995).

Associative learning linked to other sensory modalities, or success-motivated searching, as found in several hymenopteran parasitoid species (Godfray, 1993), cannot, however, be excluded as a contributor to a multimodal search strategy. The absence of olfactory and visual cues in the present experimental conditions shows that such cues are not necessary for host finding. Hence, acoustic information alone can lead the fly in her search for a cricket.

Persistence of orientation

The persistence of orientation strongly suggests that the fly is capable of gauging the direction of, and possibly the distance

to, the sound source. When acoustic cues are absent, and in the absence of other cues, it is tempting to surmise that past acoustic information must be used, or retrieved, for the fly to home in on the loudspeaker. Supporting this strong claim phenomenologically is the fact that the fly's landing accuracy on the inactive loudspeaker decreases with increasing distance from the loudspeaker at stimulus interruption (Figs 8, 9). This quantitatively gradual change in phonotactic performance may have several causes. Since the fly's ability to gather positional information is likely to improve as she approaches the loudspeaker, a deficit in the accuracy of orientation (for an early stimulus interruption) could reflect the relative inaccuracy of the acquisition of acoustic information at long range. Another, non-exclusive, possibility pertains to cumulative errors in the flight motor output, in that sense lacking the acoustically driven error-correction mechanisms. The possibility that the flies are capable of acoustically gauging their distance from a sound source is very intriguing and is the subject of ongoing investigations (P. Müller and D. Robert, in preparation).

Persistence of orientation seems to be a phenomenon common to both visual and acoustic worlds. In arena experiments with walking fruit flies (*Drosophila melanogaster*), Strauss and Pichler (Strauss and Pichler, 1998) found persistence in orientation towards a visual landmark that disappeared as the flies approached it. These authors termed this persistence 'after fixation', and suggested that idiothetical information is used to maintain the walking direction after stimulus interruption. Importantly, the fruit flies were allowed to walk back and forth between two visual landmarks (Buridan's paradigm), a procedure that may have provided them with the putative idiothetical information. The situation is quite different for *Ormia ochracea* because prior experience (i.e. reaching the sound source at least once previously) is not necessary for persistence to occur.

Persistence of orientation and flight trajectories

The multiple linear regression analysis reveals that landing accuracy is independent of the flight trajectory at the time of stimulus interruption. In contrast to landing accuracy, flight speed s and curvature κ at stimulus interruption contribute weakly (Table 1) to the observed persistence. The data show that fast-moving flies and those flying along a straight path tend to fly further before initiating their spiralling descent but also that, no matter what their initial trajectory, they will find the silenced loudspeaker equally well. Hence, this analysis shows that the observed persistence is not related to, and reflected in, the physical parameters of the trajectory at the time of stimulus interruption.

In all the trajectories analysed, the error angle ε increased dramatically within approximately 1 m of the sound source. Similar changes in ε have been observed for the odour-tracking behaviour of *Nautilus pompilius* (Basil et al., 2000) and of the lobster *Homarus americanus* (Moore et al., 1991) as they approach an odour source within a certain distance. In lobsters, this final increase in ε corresponds to the transition between olfactory plume-tracking and food-tasting mediated by receptors on the legs (Moore et al., 1991); in *Nautilus pompilius*, the receptors are located on the tentacles (Basil et al., 2000). In *Ormia ochracea*, the transition in the distribution of error angles takes place as the fly initiates the landing phase (Fig. 5D–F). Whether this change is a cause or an effect of the landing behaviour is, of course, a conundrum to be resolved. It is remarkable, however, that the loudspeaker can be found when stimulus interruptions take place at distances at which error angles are small. Thus, whilst it is possible in theory to use ε to estimate distance and position, the multiple linear regression analysis shows that ε is not a predictor of either landing accuracy or persistence of orientation.

Ultimately, at the level of perception, the information used by the fly must be derived from some acoustic variables of the cricket's calling song. Such variables are not infinitely diverse and must relate somehow to amplitude, frequency and time information contained in the sound wave. Other dynamic combinations of these fundamental variables, such as the time derivatives of frequency and amplitude, may also be relevant. Using the system of on-line stimulus control described here, our current work examines phonotactic trajectories in response to a variety of stimulus variables likely to convey information about the direction and distance of the sound source (P. Müller and D. Robert, in preparation).

Avoidance of parasitism by song interruption

The persistence of orientation after stimulus interruption demonstrates the fly's capacity to pursue a temporarily silent host. In nature, crickets such as *Gryllus rubens* temporarily interrupt their trilling song (Doherty and Callos, 1991). In the nocturnal bushcricket species *Neoconocephalus ensiger*, stridulating males that encounter a disturbance perform a variety of anti-predator behaviours, such as song cessation, freezing, diving, jumping and evasive flight (Faure and Hoy, 2000). Song cessation and pausing in katytids are behavioural patterns that can be elicited by exposure to pulsed ultrasound. Similarly, the question whether the fly's flight tone (200–400 Hz) can elicit song cessation in crickets remains open. The high sensitivity of the cricket's cercal wind receptors (Kumagai et al., 1998) might prove suitable for the early detection of an approaching fly. The evidence gathered so far establishes that low-frequency air puffs (10–50 Hz) directed at the abdominal cerci elicit a running escape response (Gras and Hörner, 1992; Gnatzy and Kämper, 1990). According to the present results, crickets should be able to detect an approaching fly early enough (more than 1.5 m away) to reduce, through song cessation, their conspicuousness. Hence, persistence in the fly's phonotaxis ought to exert an important influence on the cricket's ability to avoid acoustic parasitism. The present results also corroborate the finding (Walker, 1993) that the omission of as many as half of the pulses in the simulated calling song of *G. rubens* did not significantly reduce captures of *O. ochracea* at sound traps. Accordingly, chirping or stuttering (i.e. the

production of songs with sound pulses in short or irregular groups) seems to be no safeguard against the acoustic parasitoid. Further investigations on the efficiency of phonotaxis as a function of the fine structure, variability and quality of a cricket's song will contribute to a better understanding of the co-evolution of cricket signalling and fly hearing.

Table of symbols

FHF	finite helix fit
V	translational velocity
T	unit tangent vector
s	speed
κ	curvature
τ	torsion
w	dimensionless window size
α	actual angle
ε	error angle
$\lvert\varepsilon\rvert$	absolute error angle
δ	residual angle

The authors thank Hanni Kohler for rearing the animals, Hansjörg Baumann for his invaluable support in programming LabVIEW applications and Martin Bichsel, Steven Fry, Helmut Heise and Stephan Hischier for developing the software and hardware of the tracking system. This research was supported by grants from the Swiss National Science Foundation and the Claraz Donation to D.R.

References

Adamo, S. A., Robert, D., Perez, J. and Hoy, R. R. (1995). The response of an insect parasitoid, *Ormia ochracea* (Tachinidae), to the uncertainty of larval success during infestation. *Behav. Ecol. Sociobiol.* **36**, 111–118.

Azzalani, A. and Chiogna, M. (1995). *rm.tools: Some S-Plus Tools for the Exploratory and Parametric Analysis of Repeated Measures Data*. Report no. 4, Università di Padova, Italia.

Basil, J. A., Hanlon, R. T., Sheikh, S. I. and Atema, J. (2000). Three-dimensional odor tracking by *Nautilus pompilius*. *J. Exp. Biol.* **203**, 1409–1414.

Batschelet, E. (1981). *Circular Statistics in Biology*. London: Academic Press.

Cade, W. (1975). Acoustically orienting parasitoids: fly phonotaxis to cricket song. *Science* **190**, 1312–1313.

Crenshaw, H. C., Ciampaglio, C. N. and McHenry, N. (2000). Analysis of the three-dimensional trajectories of organisms: estimates of velocity, curvature and torsion from positional information. *J. Exp. Biol.* **203**, 961–982.

Doherty, J. A. and Callos, J. D. (1991). Acoustic communication in the trilling field cricket, *Gryllus rubens* (Orthoptera: Gryllidae). *J. Insect Behav.* **4**, 67–82.

Edgecomb, R. S., Robert, D., Read, M. P. and Hoy, R. R. (1995). The tympanal hearing organ of a fly: phylogenetic analysis of its morphological origins. *Cell Tissue Res.* **282**, 251–268.

Faure, P. A. and Hoy, R. R. (2000). The sounds of silence: cessation of singing and song pausing are ultrasound-induced acoustic startle behaviors in the katydid *Neoconocephalus ensiger* (Orthoptera; Tettigonidae). *J. Comp. Physiol.* A **186**, 129–142.

Fry, S. N., Bichsel, M., Müller, P. and Robert, D. (2000). Tracking of flying insects using pan-tilt cameras. *J. Neurosci. Meth.* **101**, 59–67.

Gnatzy, W. and Kämper, G. (1990). Digger wasp against crickets. II. An airborne signal produced by a running predator. *J. Comp. Physiol.* A **167**, 551–556.

Godfray, H. C. J. (1993). *Parasitoids: Behavioural and Evolutionary Ecology*. Princeton: Princeton University Press.

Gras, H. and Hörner, M. (1992). Wind-evoked escape running of the cricket *Gryllus bimaculatus*. I. Behavioural analysis. *J. Exp. Biol.* **171**, 189–214.

Hischier, S. (1999). Host-finding in the parasitoid fly *Ormia ochracea* (Diptera: Tachinidae: Ormiini): a 2-D flight-trajectory analysis. Diploma thesis, University of Zurich.

Kumagai, T., Shimozawa, T. and Baba, Y. (1998). Mobilities of the cercal wind-receptor hairs of the cricket, *Gryllus bimaculatus*. *J. Comp. Physiol.* A **183**, 7–21.

Lakes-Harlan, R. and Heller, K.-G. (1992). Ultrasound-sensitive ears in a parasitoid fly. *Naturwissenschaften* **79**, 224–226.

Lehmann, G. U. C. and Heller, K.-G. (1998). Bushcricket song structure and predation by the acoustically orienting parasitoid fly *Therobia leonidei* (Diptera: Tachinidae: Ormiini). *Behav. Ecol. Sociobiol.* **43**, 239–245.

Michelsen, A. and Rohrseitz, K. (1997). Sound localisation in a habitat: an analytical approach to quantifying the degradation of directional cues. *Bioacoustics* **7**, 291–313.

Miles, R. N., Robert, D. and Hoy, R. R. (1995). Mechanically coupled ears for directional hearing in the parasitoid fly *Ormia ochracea*. *J. Acoust. Soc. Am.* **98**, 3059–3070.

Moore, P. A., Scholz, N. and Atema, J. (1991). Chemical orientation of lobsters, *Homarus americanus*, in turbulent odor plumes. *J. Chem. Ecol.* **17**, 1293–1307.

Ramsauer, N. and Robert, D. (2000). Free-flight phonotaxis in a parasitoid fly: behavioural thresholds, relative attraction and susceptibility to noise. *Naturwissenschaften* **87**, 315–319.

Robert, D., Amoroso, J. and Hoy, R. R. (1992). The evolutionary convergence of hearing in a parasitoid fly and its cricket host. *Science* **258**, 1135–1137.

Robert, D. and Hoy, R. R. (1998). The evolutionary innovation of tympanal hearing in Diptera. In *Comparative Hearing: Insects* (ed. R. R. Hoy, A. N. Popper and R. R. Fay), pp. 197–227. New York: Springer-Verlag.

Robert, D., Miles, R. N. and Hoy, R. R. (1996). Directional hearing by mechanical coupling in the parasitoid fly *Ormia ochracea*. *J. Comp. Physiol.* A **179**, 29–44.

Robert, D., Miles, R. N. and Hoy, R. R. (1998). Tympanal mechanics in the parasitoid fly *Ormia ochracea*: intertympanal coupling during mechanical vibration. *J. Comp. Physiol.* A **183**, 443–452.

Robert, D., Read, M. P. and Hoy, R. R. (1994). The tympanal hearing organ of the parasitoid fly *Ormia ochracea* (Diptera, Tachinidae, Omiini). *Cell Tissue Res.* **275**, 63–78.

Römer, H. (1998). The sensory ecology of acoustic communication in insects. In *Comparative Hearing: Insects* (ed. R. R. Hoy, A. N. Popper and R. R. Fay), pp. 63–96. New York: Springer-Verlag.

Strauss, R. and Pichler, J. (1998). Persistence of orientation toward a temporarily invisible landmark in *Drosophila melanogaster*. *J. Comp. Physiol.* A **182**, 411–423.

Venables, W. N. and Ripley, B. D. (1997). *Modern Applied Statistics with S-Plus*. Second edition. New York: Springer-Verlag.

Wagner, W. E. (1995). Convergent song preferences between female field crickets and acoustically orienting parasitoid flies. *Behav. Ecol.* **7**, 279–285.

Walker, T. J. (1986). Monitoring the flights of field crickets (*Gryllus* spp.) and a tachinid fly (*Euphasiopterix ochracea*) in north Florida. *Florida Ent.* **69**, 685–685.

Walker, T. J. (1993). Phonotaxis in female *Ormia ochracea* (Diptera: Tachinidae), a parasitoid of field crickets. *J. Insect Behav.* **6**, 389–410.

Zuk, M., Rotenberry, J. T. and Simmons, L. W. (1997). Calling songs of field crickets (*Teleogryllus oceanicus*) with and without phonotactic parasitoid infection. *Evolution* **52**, 166–171.

Zuk, M., Simmons, L. W. and Cupp, L. (1993). Calling characteristics of parasitized and unparasitized populations of the field cricket *Telleogryllus oceanicus*. *Behav. Ecol. Sociobiol.* **33**, 339–343.